The Time Course of Activity in Dorsolateral Prefrontal Cortex and Anterior Cingulate Cortex during Top-Down Attentional Control

Rebecca Levin Silton,
University of Illinois at Urbana-Champaign

Wendy Heller,
University of Illinois at Urbana-Champaign

David N. Towers,
University of Illinois at Urbana-Champaign

Anna S. Engels,
University of Illinois at Urbana-Champaign

Jeffrey M. Spielberg,
University of Illinois at Urbana-Champaign

J. Christopher Edgar,
University of Illinois at Urbana-Champaign

Sarah M. Sass,
University of Illinois at Urbana-Champaign

Jennifer L. Stewart,
University of Illinois at Urbana-Champaign

Bradley P. Sutton,
University of Illinois at Urbana-Champaign

Correspondence concerning this article should be addressed to Wendy Heller or Gregory A. Miller, Department of Psychology, University of Illinois, Champaign, IL 61820. w-heller@illinois.edu or gamiller@illinois.edu.

Rebecca Levin Silton, Department of Psychology, University of Illinois at Urbana-Champaign; Wendy Heller, Department of Psychology and Beckman Institute Biomedical Imaging Center, University of Illinois at Urbana-Champaign; David N. Towers, Department of Psychology, University of Illinois at Urbana-Champaign; Anna S. Engels, Department of Psychology, University of Illinois at Urbana-Champaign; Jeffrey M. Spielberg, Department of Psychology, University of Illinois at Urbana-Champaign; J. Christopher Edgar, Department of Psychology and Beckman Institute Biomedical Imaging Center, University of Illinois at Urbana-Champaign; Sarah M. Sass, Department of Psychology, University of Illinois at Urbana-Champaign; Jennifer L. Stewart, Department of Psychology, University of Illinois at Urbana-Champaign; Bradley P. Sutton, Department of Psychology and Beckman Institute Biomedical Imaging Center, University of Illinois at Urbana-Champaign; Marie T. Banich, Institute of Cognitive Science, and Department of Psychology and Neuroscience, University of Colorado; Gregory A. Miller, Departments of Psychology and Psychiatry and Beckman Institute Biomedical Imaging Center, University of Illinois at Urbana-Champaign.

Rebecca Levin Silton is now at Department of Child and Adolescent Psychiatry and Behavioral Medicine, Seattle Children's Hospital; Anna S. Engels is now at Department of Psychology and Social, Life, and Engineering Sciences Imaging Center, Pennsylvania State University; J. Christopher Edgar is now at Department of Radiology, The Children's Hospital of Philadelphia; Jennifer L. Stewart is now at Department of Psychology, University of Arizona

Marie T. Banich, and
University of Colorado at Boulder

Gregory A. Miller
University of Illinois at Urbana-Champaign

Abstract

A network of brain regions has been implicated in top-down attentional control, including left dorsolateral prefrontal cortex (LDLPFC) and dorsal anterior cingulate cortex (dACC). The present experiment evaluated predictions of the cascade-of-control model (Banich, 2009), which predicts that during attentionally-demanding tasks, LDLPFC imposes a top-down attentional set which precedes late-stage selection performed by dACC. Furthermore, the cascade-of-control model argues that dACC must increase its activity to compensate when top-down control by LDLPFC is poor. The present study tested these hypotheses using fMRI and dense-array ERP data collected from the same 80 participants in separate sessions. fMRI results guided ERP source modeling to characterize the time course of activity in LDLPFC and dACC. As predicted, dACC activity subsequent to LDLPFC activity distinguished congruent and incongruent conditions on the Stroop task. Furthermore, when LDLPFC activity was low, the level of dACC activity was related to performance outcome. These results demonstrate that dACC responds to attentional demand in a flexible manner that is dependent on the level of LDLPFC activity earlier in a trial. Overall, results were consistent with the temporal course of regional brain function proposed by the cascade-of-control model.

A network of brain regions supports top-down attentional control (Banich, 2009; Banich et al., 2009; Banich et al., 2000a, 2000b; Buschman & Miller, 2007; Kerns, et al., 2004; Liu, Banich, Jacobson, & Tanabe, 2006; MacDonald, Cohen, Stenger, & Carter, 2000; Miller & Cohen, 2001). A number of functional magnetic resonance imaging (fMRI) and positron-emission tomography (PET) studies have identified left dorsal lateral prefrontal cortex (LDLPFC) and dorsal anterior cingulate cortex (dACC) as key brain regions that initiate and monitor the need for top-down attentional control and adjust performance based on contextual demands (Banich et al., 2000b; Botvinick, Cohen, & Carter, 2004; Carter, Botvinick, & Cohen, 2007; Cohen, Botvinick, & Carter, 2000; MacDonald et al., 2000; Milham, Banich, & Barad, 2003). Although these findings are robust, few studies have evaluated the time course of relevant activity in these brain regions during attentional control tasks, in part because fMRI and PET provide limited temporal resolution.

Research investigating the time course of attentional control in healthy controls has relied largely on scalp event-related brain potential (ERP) methods (Donkers & van Boxtel, 2004; Holroyd, 2004; Jackson, Jackson, Roberts, 1999; Kiefer, Marzinzik, Weisbrod, Scherg, & Spitzer, 1998; Liotti, Woldorff, Perez, & Mayberg, 2000; West, 2003; West, Bowry, & McConville, 2004). Scalp ERP methods have temporal resolution on the order of milliseconds, but this temporal resolution often comes at the expense of spatial resolution. To date, no known study has integrated hemodynamic and electrocortical methods to identify the time course of regional brain activity associated with top-down attentional control. Such an approach has great potential to advance theories of attentional control.

Identifying the temporal course of activity in brain regions implicated in attentional control is crucial to improving understanding of the individual roles of these brain regions as well as how they function in conjunction as a network and how they may go awry in mental illness.

fMRI and PET studies employing the color-word Stroop task (e.g., Stroop, 1935) have offered some insight into the role and time course of LDLPFC and dACC during top-down attentional control (Banich, 2009; Botvinick, Cohn, & Carter, 2004; Kerns et al., 2004). The "Stroop interference effect" refers to a typical response pattern involving longer reaction time (RT) following incongruent stimuli (the word "red" in blue ink) than congruent (the word "red" in red ink) or neutral stimuli (a non-word such as "XXXX" or a non-color word, such as "bond", in red ink). MacDonald et al. (2000) examined brain activity for incongruent stimuli when the color had to be named, which requires an override of the more automatic process of word reading. They found more LDLPFC activity for color naming than for word reading. Banich et al. (2000a) found activation of bilateral DLPFC regions in both a standard color-word Stroop and a spatial-word Stroop task, indicating engagement of this region regardless of whether the task-relevant feature was an item's color or its spatial location. Furthermore, they found that this effect did not vary depending on the type of information to be ignored, as DLPFC was activated both for a color-word Stroop task and for a color-object Stroop task. Similarly, Fan et al. (2003) showed that LDLPFC was activated during both the Stroop task and the Spatial Conflict task (which involved nonverbal stimuli). Banich et al. (2000b) proposed that DLPFC provides a top-down attentional set toward task-relevant information and processes (e.g., ink-color identification). Although presumably such an attentional set would be imposed early on in the course of activity, this hypothesis has not been explicitly tested with data that can precisely address the temporal course of LDLPFC activity.

Beginning with the work of Pardo, Pardo, Janer, and Raichle (1990), much hemodynamic neuroimaging research has emphasized the role of ACC during Stroop performance (e.g., Botvinick, Braver, Barch, Carter, & Cohen, 2001; Botvinick et al., 2004; Casey, Tottenham, & Fossella, 2002; MacDonald et al., 2000; Mohanty et al., 2007). Pardo et al. (1990) found more ACC activity during incongruent than congruent trials. This result has been replicated using a comparison between incongruent and congruent conditions (Carter, Mintun, & Cohen, 1995) as well as incongruent and neutral conditions (Bench et al., 1993). MacDonald et al. (2000) reported that participants who showed more Stroop interference tended to have more dACC activity and that dACC, but not LDLPFC, distinguished incongruent and congruent trials. These findings have encouraged theorizing about the role of the dACC during tasks that involve high levels of conflict that demand resolution (Botvinick et al., 2001, 2004). However, the precise roles of LDLPFC and dACC remain uncertain, in part due to the paucity of relevant time-course information for regional brain activity.

The cascade-of-control (cascade) model proposes that DLPFC guides top-down attentional processing, and later dACC activity is thought to be involved in resolving response-related attentional processes (Banich, 2009; Liu et al., 2006; Milham et al., 2001, 2003; Milham & Banich, 2005). Using a variant of the Stroop task, Milham et al. (2001) found that dACC was activated when the word identified an ink color that represented an alternative (conflicting) response, but not when the word identified an ink color that was not a possible

response (the word conflicted with regard to semantics, but not with regard to a response). Further evidence for a dissociation between DLPFC and dACC was provided by Liu et al. (2006), who found that, unlike dACC activity, DLPFC activity was relatively impervious to whether a particular word was mapped to one or more responses. These findings are in accord with the view that, within a trial, DLPFC takes a dominant early role in top-down attentional control and that dACC is involved in later stages of selection that are linked to response-related processes (Liu et al., 2006).

ERP source analysis offers a promising method to evaluate the time course of DLPFC and dACC activity during the Stroop task. Scalp ERP color-word Stroop studies have been inconsistent, with an N400 component emerging most often (some color-word Stroop studies have referred to this component as the N450). N400 has been characterized as a distributed scalp ERP component (latency 400 ms to 500 ms) that is larger (more negative) during incongruent than during congruent trials (Hanslmayr et al., 2008; Holmes & Pizzagalli, 2008; Liotti et al., 2000; Markela-Lerenc et al., 2004). N400 is thought to reflect dACC activity and has been theorized to be related to processes occurring at the response stage (Hanslmayr et al., 2008; Holmes & Pizzagalli, 2008; Liotti et al., 2000; West et al., 2004). It remains unclear whether this component is the same as the classic N400 first identified by Kutas & Hillyard (1980).

An earlier component, N200, has sometimes been reported in the color-word Stroop (Holmes & Pizzagalli, 2008) and other visual interference tasks. This negative, frontally distributed component is thought to be generated by inferior/lateral PFC (Jackson, et al., 1999; Kiefer et al., 1998) or dACC (van Veen & Carter, 2002, Yeung, Botvinick, & Cohen, 2004). N200 has also been associated with conflict monitoring (Donkers & van Boxtel, 2004; Holmes & Pizzagalli, 2008; Yeung et al., 2004). The exact process that is being indexed by this very early potential remains unclear.

Several recent studies have used ERP source analysis with Stroop data (Badzakova-Trajkov, Barnett, Waldie, & Kirk, 2009; Hanslymayer et al., 2008; Holmes & Pizzagalli, 2008; Liotti et al., 2000; Markela-Lerenc et al., 2004; West, 2003; West et al., 2004). Source analyses point to dACC activity occurring at 400 ms to 500 ms (Badzakova-Trajkov, 2009; Hanslmayr et al., 2008; Holmes & Pizzagalli, 2008; Liotti et al., 2000; Markela-Lerenc et al., 2004). Liotti et al. (2000) used coordinates from Pardo et al.'s (1990) PET study to position a dACC dipole, while allowing the orientation of the dipole to vary. This dipole accounted for 85% of the variance at the peak of the activity (410 ms). Similarly, Hanslmayr et al. (2008) reported peak activity around 400 ms for dACC.

Markela-Lerenc et al. (2004) conducted source analysis using a difference waveform (incongruent- minus congruent-trial waveforms) in an attempt to isolate the processes specifically associated with the interference effect. They fit a model that involved a left PFC dipole and an ACC dipole. Somewhat supporting the cascade model, left PFC was maximally active at 400 ms, and ACC was maximally active at 470 ms. However, visual inspection of their published dipole waveforms suggests that the two dipoles may be redundant and that their model is better fit with a single dipole. Badzakova-Trajkov et al. (2009) also used a difference source waveform comparison method, identifying a dACC

peak at 425 ms for the incongruent-congruent difference waveform, which is consistent with the findings from the other Stroop source analysis studies. However, source analysis performed on difference waveforms is problematic, since the subtraction method involved in calculating this waveform will tend to distort the scalp topography, which could result in compromised dipole locations and time courses. Source analyses that were based on a difference waveform should therefore be interpreted cautiously. To avoid such problems, the present study did not use difference waveforms.

Despite variance in participant selection, experimental design, and source analysis strategies, the converging findings are encouraging and suggest a robust effect likely related to dACC activity that occurs between 400 ms to 500 ms. This is also consistent with scalp ERP findings. This later dACC activity is likely related to later aspects of response selection, rather than earlier aspects of conflict monitoring, which would be expected to occur possibly as early as 200 ms. Overall, the temporal pattern of data revealed in the ERP literature provides strong support for the plausibility of the cascade model, but a more definitive test is needed.

The present study sought to resolve the question of the relative timing and magnitude of LDLPFC and dACC activity associated with top-down attentional control processes in the course of a trial by using the power afforded by the parallel acquisition of fMRI and ERP data. These data were obtained in separate sessions for a large set of 80 carefully screen undergraduate student while they performed the attentionally-demanding Stroop task. The scalp ERP data were analyzed to a limited degree with the sole purpose of replicating previous findings in order to show that the scalp topography is consistent with previous studies prior to moving forward with source analysis.

Of importance for the present hypotheses and different from prior studies, the fMRI data were used to guide the placement of ERP sources. These data were then examined to determine whether they would support a temporal pattern consistent with the cascade-of-control model. In addition, the present study examined how activity was related to overt behavior. Mediation analyses were used to evaluate the time-course of the relationship between LDLPFC and dACC as predicted by the cascade model (see Figure 1). Based on available ERP data, it was hypothesized that the mediation analyses would support a temporal pattern consistent with the cascade model, which argues that the influence of LDLPFC on behavioral performance would be mediated by late-stage activity in dACC.

Materials and Methods

Participants

Participants ($N = 89$, 44% female, 78% Caucasian) were paid volunteers age 18–34 (M = 19.2, SD = 1.9) recruited from introductory psychology classes via group questionnaire screening sessions. Nine participants were considered outliers on ERP measures (3 SD from the mean for at least one component) and were omitted from subsequent analyses. The participants were right-handed as determined by the Edinburgh Handedness Inventory (Oldfield, 1971) and were native English speakers. Since psychoactive medications are known to affect executive function and related regional brain activity (Brody et al., 2001;

Kennedy et al., 2001), participants were screened by self-report to be free of such medications. Participants were also screened for abnormal color vision, loss of consciousness > 10 minutes, claustrophobia, recent drug/alcohol use, excessive caffeine intake, and lack of sleep. Participants were given a laboratory tour, were informed of the study procedures, and provided written consent.

Since the participants included in this study were part of a larger project examining the impact of psychopathology on attentional control, participants completed the Penn State Worry Questionnaire (PSWQ; Meyer, Miller, Metzger, & Borkovec, 1990; Molina & Borkovec, 1994) and parts of the Mood and Anxiety Symptom Questionnaire (Anxious Arousal scale, MASQ-AA; Anhedonic Depression 8-item depressed mood subscale, MASQ-AD-8; Nitschke, Heller, Imig, McDonald, & Miller, 2001; Watson et al., 1995a, 1995b). Participants scored either above the 80th percentile on at least one of these scales or below the 50th percentile on all three. The Structured Clinical Interview for Axis I Disorders, Non-patient edition (First, Spitzer, Gibbon, & Williams, 1997), was also administered to assess Axis I disorders. Lifetime DSM-IV diagnoses were determined by the interviewer and reviewed by a consensus team consisting of a second interviewer and a clinical faculty supervisor (GAM) on the scale: 1 = absent, 2 = features (at least 2 symptoms), 3 = provisional (1 short of full DSM-IV criteria), and 4 = definite. This information about psychopathology guided selection for this report of a group of participants representative of a typical college sample from the larger sample recruited for ongoing studies. Based on a sample of 2188 college students, Blanco et al. (2008) reported that 20% of their sample met DSM-IV criteria for either an anxiety or depressive disorder within the past 12 months. Comparably, 26% of the present sample met DSM-IV criteria for lifetime diagnoses of either anxiety (e.g., Panic Disorder, Social Phobia, Specific Phobia, OCD, PTSD, Acute Stress Disorder, GAD, anxiety NOS) and/or depressive disorder (e.g., MDD, Dysthymia, Depressive Disorder NOS). None of the participants was currently in a Major Depressive Episode.

Stimuli and Experimental Design

Participants completed an emotion-word Stroop task and a color-word Stroop task. Both tasks were administered during an fMRI session and an electroencephalography (EEG) session. The order of presentation of the two Stroop tasks within a session was counterbalanced across participants, as was the order of the EEG and fMRI sessions, with the SCID session in-between for most participants. The emotion-word Stroop data do not address present goals and will not be considered further here. The color-word Stroop task consisted of blocks of color-congruent or color-incongruent words alternating with blocks of neutral words, with 256 trials in 16 blocks (4 color-congruent, 4 color-incongruent, 8 neutral). Half the trials in congruent and incongruent blocks were neutral, to prevent the development of word-reading strategies. There were eight orders of stimulus presentation for each Stroop task, designed specifically to control stimulus order effects. Each participant received one of the eight orders.

Each trial consisted of one word presented in one of four ink colors (red, yellow, green, blue). Trials began with the presentation of a word for 1500 ms, followed by a fixation cross

for 275 ms to 725 ms (onset to onset ITI 2000 +/− 225 ms). Word presentation and response recording were controlled by STIM software (James Long Company, Caroga Lake, NY). In the fMRI session, words were presented in capital letters using Tahoma 72-point font via backprojection onto a screen outside the scanner bore and a mirror fixed to the head coil, providing a vertical span of 2.9 degrees, and a horizontal span of 6.1 – 16.4 degrees. In the ERP session, the same words were presented on a CRT monitor 1.35 m from the participants' eyes, for a vertical span of 1.5 degrees and a horizontal span of 3.2 – 8.7 degrees. Participants responded with their middle and index fingers, with each task using the same mapping of color to button. There was a color-to-key-mapping acquisition phase of 32 practice trials. In addition to the 16 word blocks, there were four fixation blocks – one at the beginning, one at the end, and two in the middle of the session. In the fixation condition, a brightened fixation cross was presented for 1500 ms.

MRI Recording, Data Reduction, and Analysis

Thirty participants who did not have a history of psychopathology were included in fMRI analyses that were used to identify brain regions active during the color-word Stroop task in order to guide the placement of sources in the ERP source model. An improved fMRI acquisition protocol was implemented after data collection for this study began, and 35 participants without a psychopathology history were run through the new protocol. Only fMRI data collected under the new fMRI protocol for these 30 participants were analyzed, providing guidance for the ERP source analysis that was carried out for all 80 participants. Two participants who met criteria for fMRI analyses were excluded due to excessive motion, and three participants were excluded due to other artifact, leaving the final $N = 30$.

The MR technologist and experimenter assisted the participant in correct placement of earplugs and protective headphones. MR data were collected using a research-dedicated 3T Siemens Allegra. Three hundred and seventy functional images were acquired using a gradient-echo echo-planar imaging (EPI) sequence (TR 2000 ms, TE 25 ms, flip angle 80°, FOV = 22 cm). Thirty-eight contiguous oblique axial slices (slice thickness 3 mm, in-plane resolution 3.4375×3.4375 mm^2, .3 mm gap between slices) were acquired parallel to the anterior and posterior commissures. After the EPI sequence, a 160-slice MPRAGE structural sequence was acquired (slice thickness 1 mm, in-plane resolution 1×1 mm) for registering each participant's functional data to standard space.

Image processing and analyses relied primarily on tools from the FSL analysis package (e.g., MCFLIRT, FNIRT, PRELUDE, FILM, FUGUE, FEAT, FLAME; http://www.fmrib.ox.ac.uk/fsl). Each fMRI time series was first motion-corrected using MCFLIRT (Jenkinson, Bannister, Brady, & Smith, 2002), and spikes (artifactual sudden intensity shifts) were corrected using the AFNI tool 3d Despike (http://afni.nimh.nih.gov/afni). All participants demonstrated less than 3.3 mm absolute motion or 2 mm relative motion (participants with motion exceeding this threshold were excluded from analysis, beyond the 30 control participants relied on in the present analysis). After motion correction and despiking, each time series was corrected for geometric distortions caused by magnetic field inhomogeneity. Remaining preprocessing steps, single-subject statistics, and group statistics were implemented by FEAT. The first 3 volumes of each dataset were discarded to allow the

MR signal to reach a steady state. Each time series was then temporally filtered with a nonlinear high-pass filter (to remove drift in signal intensity), mean-based intensity-normalized by the same single scaling factor, and spatially smoothed using a 3D Gaussian kernel (full-width-half-maximum 5 mm) prior to analysis.

Regression analyses were performed on each participant's time series using FILM. Statistical maps were generated via multiple regression computed for each intracerebral voxel (Woolrich, Ripley, Brady, & Smith, 2001). An explanatory variable (EV) was created for each block type (color-congruent, color-incongruent, neutral, rest), with the fixation condition the unmodeled baseline. Each EV was convolved with a gamma function to better approximate the temporal course of the blood-oxygen-dependent (BOLD) hemodynamic response (e.g., Aguirre, Zarahn, & D'Esposito, 1998; Miezin, Maccotta, Ollinger, Petersen, & Buckner, 2000). Each EV yielded a per-voxel effect-size parameter (β) estimate (PE) map representing the magnitude of activity associated with that EV. The β values for the incongruent word condition were contrasted with those for the congruent word condition, resulting in a per-voxel contrast parameter estimate map for each participant. These functional activation maps as well as the corresponding structural MRI map were registered into Montreal Neurological Institute (MNI) stereotaxic space using FNIRT with FSL's default configuration file and a warp resolution of 10 mm.

Inferential statistical analyses were carried out using FLAME. To identify regions associated with the Stroop interference effect, significantly activated voxels were identified for the incongruent minus congruent contrast via a one-sample t-test, yielding a 3D functional z-map image. Monte Carlo simulations via AFNI's AlphaSim program (Ward, 2000) estimated the overall significance level (probability of a false detection) for thresholding, using a gray-matter mask to limit the number of voxels under consideration. These simulations provided a z-value (z = 3.0902, p = .01) and cluster size (34 voxels) combination for thresholding that resulted in an overall familywise error rate of .05. Clusters that survived this thresholding are reported in Table 1. Center of Mass coordinates for clusters in hypothesized regions of interest were used to place regional sources in the ERP source model.

Electrophysiological Recording, Data Reduction, and Analysis

Participants were seated in a comfortable chair in a quiet room connected to the adjacent equipment room by intercom. EEG was recorded with a custom-designed Falk Minow 64-channel cap with equidistantly spaced Ag/AgCl electrodes. After placement of the electrode cap, electrode positions were digitized for later topographic and source-localization analyses. By placing electrodes above and below each eye and near the outer canthus of each eye, horizontal and vertical EOG were recorded for off-line eye-blink artifact correction of the EEG data implemented in BESA 5.1.8 (Berg & Scherg,1994). The left mastoid served as the online reference for all sites. Impedances were below 20 kΩ, appropriate given the high input impedance of the amplifiers. Half-power amplifier bandpass was .1 to 100 Hz, with digitization at 250 Hz.

The following steps were done separately for each participant. Muscle and other artifact was manually removed using BESA 5.1.8. A series of steps were taken to remove and/or correct

eye blinks and eye movements. First, bipolar channels were created to examine both vertical and horizontal eye movement (EEG channels above and below both the right and left eye to examine vertical eye movement, and EEG channels near the left and right external canthi to examine horizontal eye movements). Examining these bipolar channels, epochs where either a horizontal or vertical saccade was identified were marked as artifact periods and removed from the data (there were not enough vertical or horizontal saccades to create an average of either saccade type). Second, a typical blink was identified in the data. Using the pattern search function in BESA, the data were scanned to identify all blink periods. The marker identifying each blink was set to the middle of each blink. The BESA pattern function scanned the entire time series, calculating the correlation between the user-defined pattern and all other time periods (the correlation threshold was set to .50).

Once other blinks were identified, all blinks were averaged. Stimulus-locked averages were also calculated for each of the experimental conditions (congruent, incongruent, and neutral) for each participant. The EEG data remained in 59-channel space for source analysis. However, for ERP scalp analyses, the condition averages and blink averages were interpolated to BESA's standard 81-channel configuration using spherical spline interpolation and placed according to the 10–10 system (Perrin, Pernier, & Bertrand, 1989), facilitating comparison with other studies. Electrode voltages were re-referenced to an average-reference montage that was computed for each time point as the mean voltage over the interpolated amplitudes of the 81 standard virtual scalp electrodes. Only trials with correct responses that occurred within 350–1400 ms were included. Only participants who had a minimum of 16 trials per each condition average were included in analyses. All 89 participants met these criteria.

Following these steps, the surrogate multiple source eye correction (MSEC) algorithm was used to correct blink artifacts for each participant (Berg & Scherg, 1994). This method differs from traditional artifact correction routines. In traditional methods (e.g., Miller, Gratton, & Yee, 1988), a measure of eye movement or blink activity at horizontal and vertical electrode sites is obtained, transmission coefficients across the head are estimated, and the site-specific fraction of the EOG is subtracted from all other EEG sites. A limitation of this method is that activity from the brain that is contained in the EOG channels is also subtracted, removing both eye artifact and brain signal, especially at frontal sites. In the MSEC method, using all EEG channels, sources of artifact (e.g., blink) and brain activity are simultaneously modeled, and only the modeled blink activity is removed from each EEG channel. The advantage of the MSEC method is reduced distortion of brain activity by accounting for the EEG signal during the estimation of eye activity. In order to apply the MSEC method, the blink source vector was selected as the component with the maximum variance for each participant (typically over 99%). The standardized set of surrogate brain sources available in BESA 5.1.8, was temporarily used to model brain activity along with blink activity. The surrogate brain sources were not used in subsequent analyses.

The scalp ERP component analysis method computed the cross-trial average ERP associated with stimulus presentation for each participant. Data were exported from BESA and baseline-adjusted by subtracting the average amplitude for the 200 ms before stimulus onset. W1aveform averages were smoothed using a 101-weight, .1–12 Hz (half-amplitude) digital

filter (Cook & Miller, 1992; Edgar, Stewart, & Miller, 2005; Nitschke, Miller, & Cook, 1998). Amplitude and latency scores were obtained for ERP components at each of the 81 virtual electrodes. Choices of electrode sites as well as specific scoring windows were determined on the basis of present data and previous ERP research that investigated these components. Thus, N200 (220 ms to 340 ms) and N400 (400 ms to 600 ms) were scored. Electrode Cz was used in N200 and N400 amplitude analyses. Amplitude was calculated by averaging data points 24 ms before and 24 ms after peak latency, rather than just at the peak latency, in order to obtain a more reliable measure of ERP amplitude (Luck, 2005). A MANOVA was conducted to test differences in average amplitude across congruent and incongruent conditions.

In addition to conventional scalp component scoring, source modeling was carried out using BESA 5.1.8. The primary goal of the source analysis was to model the temporal course of neural activations indicated by fMRI data. A source model (see Figure 2b for full model) was created by placing regional sources based on Center of Mass coordinates for clusters obtained from a group of psychopathology-free participants with usable fMRI data ($N = 30$, a subset of the ERP sample) and in line with relevant independent fMRI research (e.g., Bush, Luu, & Posner, 2000; Mohanty et al., 2007). This subset of participants did not differ from the other participants in congruent RT $F(1,88) = .00$, $p = .99$, incongruent RT $F(1,88) = .24$, $p = .62$, or total number of errors, $F(1,88) = .95$, $p = .33$. Fourteen candidate locations survived thresholding (see Table 1). If all 14 clusters were placed as sources in the model, the model would have overfit the data. Rather, the selection of sources from among these clusters was based on relevant color-word Stroop fMRI research (Michel et al., 2004).

Four of these 14 clusters (LDLPFC, dACC, right inferior gyrus, left parietal cortex) were used in the source model (see Figure 2a for fMRI images). Although analyses for the present study primarily involved LDLPFC and dACC, the full source model included right inferior gyrus (RIFG), left parietal cortex (LPC), and right parietal cortex (RPC) in order to account for variance that is thought to be contributed by these sources based on available literature. The LDLPFC and dACC locations were very similar to the locations proposed by the cascade model (Banich, 2009) as well as by others (e.g., MacDonald et al., 2000). Other, similar studies that have used nonverbal stimuli have also implicated LDLPFC and dACC, suggesting that tasks that involve top-down attentional control recruit these brain regions across stimulus types (Fan et al., 2003; Liu, Banich, Jacobson, & Tanabe, 2004). The error rate for the fMRI session was very low (see results section for details), so it is unlikely that the error trials significantly influenced brain activity in these regions, especially given the consistency with previous research. Although the incongruent block may be associated with higher tonic levels than the congruent block, it is unlikely that present data were driven by this potential confound, since the LDLPFC and dACC fMRI locations were consistent with locations previously reported across various studies that support the cascade model.

Prior to placing these sources in the model, blink activity was modeled as described above. Next, bilateral primary visual cortex sources (LOc, ROc) were localized based on correct trials from the neutral condition. The neutral condition involved the largest number of trials and was selected to maximize the signal-to-noise ratio for localization. A grand average consisting of data from all psychopathology-free participants was used for localizing the

visual sources. The epoch used for the localization was 100 ms to 188 ms, spanning primary and secondary visual cortex responses. The LOc and ROc sources were constrained to be symmetrical (see Table 1 for LOc/ROc coordinates). Finally, the LDLPFC, dACC, RIFG, and LPC sources were placed in the model along with a contralateral RPC source. Since magnitude of source activity, rather than orientation of source activity, was the primary variable of interest, all dipoles were converted to regional sources. The ERP data were digitally filtered .1–12 Hz, and the source model was applied separately in each Stroop condition (congruent, incongruent) for each participant. Prestimulus baseline activity (−200 ms to 0 ms) was removed from the source waveforms after the model was fit to each participant. Scoring windows were based on visual inspection of the source waveforms and on relevant scalp- and source-ERP color-word Stroop research. One window for LDLPFC (300 ms to 440 ms) and two windows for dACC (220 ms to 340 ms, 520 ms to 680 ms) were chosen. Again, average amplitude was calculated by averaging data points 24 ms before and 24 ms after peak latency. With the exception of determining the location and latency window of the sources, all source-analysis steps described above were performed separately for each of the 80 participants.

Mediation analyses (MacKinnon, 2008; Preacher & Hayes, 2008) were performed in order to investigate the hypothesis that the impact of LDLPFC activity on Stroop interference is mediated by dACC activity, per the cascade model. Mediation analyses can be used to evaluate temporal relationships, provided that the temporal information is available, and the model is designed appropriately (MacKinnon, 2008). Most fMRI studies are not able to test within-trial temporal relationships using mediation analysis. However, this analysis strategy is ideal for examining ERP source analysis data, since fine-grained temporal information about regional brain activity is available.

Mediation analyses involve a series of linear regressions in order to calculate various effects and their respective weights (regression coefficients). The single mediator model (see Figure 1) involves an independent variable (IV), a mediator (M), and a dependent variable (DV). Path a represents the effects of the IV on the M. Path b represents the effect of M on the DV, partialling out the effect of the IV. Path c represents the direct effect of the IV on the DV, and path c' represents the indirect effect of the IV on the DV through M. The cascade model was assessed with LDLPFC (300 ms to 440 ms) as the IV, late dACC (520 ms to 680 ms) as the M, and Stroop interference as the DV.

Overall significance of the indirect effect ($a \times b$) was determined using bootstrapped confidence intervals rather than the Sobel test (Sobel, 1982). The Sobel test assumes that the sampling distribution of the indirect effect is normally distributed, but the indirect effect has been shown to have an asymmetrical distribution in a finite sample (Preacher & Hayes, 2004, 2008). Bootstrapping is a nonparametric method that does not require the assumption of a normal distribution and thus is a preferred method for testing the indirect effect (MacKinnon, 2008; Preacher & Hayes, 2008). Based on the recommendations of Preacher and Hayes (2008), their SPSS Macro script (http://www.comm.ohio-state.edu/ahayes; indirect.sbs) was used to conduct mediation analyses by calculating a 95% bootstrap confidence interval (CI) for the indirect effect. The CIs were used to test the null hypothesis that the indirect effect was zero. Bias-corrected and accelerated (BCa) CIs were used, since

BCa CIs have been reported to perform best with regard to power and Type I error rates (for review see Preacher & Hayes, 2008). Each bootstrapping calculation involved 5000 repetitions, well above the minimum of 1000 recommended (Preacher & Hayes, 2008). Individual model paths (a, b, c, c') were interpreted in a theoretically meaningful manner, but the significance of these paths and the specific direction of the effects were not required as criteria used to determine whether a mediation effect was present. Such requirements have been shown to increase type II errors, and significant mediation has been shown to exist even in the absence of these criteria (Preacher & Hayes, 2008).

Results and Discussion

Behavioral Performance

RT analyses were conducted to confirm that the Stroop interference effect was obtained in the present sample. A MANOVA with Condition (congruent RT, incongruent RT) and Gender confirmed slower RT for incongruent than for congruent trials, $F(1,78) = 174.07$, $p < .001$ (congruent mean = 627 ms, SD = 91 ms; incongruent mean = 789 ms, SD = 137 ms). The Stroop effect did not vary by gender. Participants made more errors during the incongruent trials than the congruent trials during the ERP session, $F(1,79) = 46.69$, $p < .001$ (congruent mean = 1 error, SD = 1, incongruent mean = 2 errors; SD = 2). To be consistent with ERP analyses, errors for the ERP session were analyzed across congruent/incongruent trials only (rather than including the neutral trials in those blocks). For the fMRI session, participants made more errors during the incongruent blocks than the congruent blocks, $F(1,29) = 18.67$, $p < .001$ (congruent mean = 2 errors, SD = 2, incongruent mean = 4 errors, SD = 3). Consistent with fMRI analyses, errors during the fMRI task were analyzed for all trials within incongruent and congruent blocks, and only behavioral data from the 30 control participants used for fMRI analyses were submitted to behavioral analyses.

Scalp ERP

In order to examine the extent to which ERP data replicated previously observed N200 and N400 waveforms at Cz (e.g., Badzakova-Trajkov et al., 2009; Hanslmayr et al., 2008; Holmes & Pizzagalli, 2008; & Markela-Lerenc et al., 2004), two MANOVAs were conducted to compare congruent and incongruent amplitudes for each component (see Figure 3 for Cz ERPs). One participant had an N200 Cz ERP score that was 3 SD from the mean and was not included in the N200 analysis. As expected, N200 amplitude was more negative for incongruent trials than congruent trials, $F(1,78) = 3.11$, $p = .08$ (a two-tailed test of what is a one-tailed hypothesis, thus an effective $p = .04$). N400 amplitude was also more negative for incongruent than congruent trials, $F(1,79) = 6.59$, $p = .01$. The scalp ERP analyses confirmed that the relevant scalp waveforms obtained from the present sample were comparable to the waveforms observed in prior color-word Stroop ERP studies. Scalp ERP analyses will not be further considered here.

Source-Waveform ERP Mediation Analysis

Most analyses using ERP source-waveform data (see Figure 4) employed scores from incongruent trials only, to examine cognitive control mechanisms prompted by Stroop conflict. The results of the mediation analyses for the cascade model are presented as Model

1 in Table 2. The indirect effect was used to test directly the overall significance of the cascade model. The indirect effect was significant, supporting the proposal that the effect of LDLPFC activity on Stroop interference is mediated by later dACC activity. In other words, LDLPFC activity influences Stroop interference via its effect on dACC.

The significant mediation occurred even though LDLPFC was not significantly associated directly with Stroop interference (path c). A significant direct effect is not required for mediation to occur (Preacher & Hayes, 2008). LDLPFC was significantly associated with the Stroop effect when mediated by dACC (path c'). The pattern of a significant c' coefficient in the presence of a nonsignificant c coefficient has been referred to as a "suppressor effect" (Cheung & Lau, 2008). A suppressor effect is present when the relationship between the IV and DV is masked by the M. When M is not included in the model, the relationship between the IV and DV declines.

Since the direct effect of LDLPFC on Stroop interference was not significant for this model, a hierarchical regression was conducted to test whether the inclusion of LDLPFC added significance variance, beyond the contribution from late dACC. To further evaluate the hypothesis that dACC and LDLPFC work in conjunction rather than independently, an interaction between dACC x LDLPFC was also included. Thus, late dACC was entered as a predictor in the first step of the regression, LDLPFC was added in the second step, and their interaction was added in the third step. Stroop interference score was the DV. Late dACC alone accounted for 4% of the variance, $F(1,78) = 3.80$, $p = .06$. When both late dACC and LDLPFC were included as predictors (total variance = 9%, $F(2,77) = 4.10$, $p = .02$), LDLPFC accounted for an additional 5% of the variance ($p = .05$). The full, three-predictor model accounted for 14% of the variance $F(3,76) = 4.17$, $p = .01$, with the interaction providing a significant increment (5%, $p = .05$), supporting the hypothesis that LDLPFC and late dACC interact rather than merely operating additively. The full model controlled more variance than is commonly considered a medium effect size (14% corresponds roughly to a correlation of .39, larger than the .30 standard for a medium effect size of Cohen, 1992).

The LDLPFC x dACC interaction was plotted in order to interpret the effect (see Figure 5a). The slope was significant for low levels of LDLPFC activity $t(76) = 3.21$, $p < .001$, but not for high levels of LDLPFC activity, $t(76) = .11$, $p = .91$. At low levels of LDLPFC activity, Stroop interference increased when dACC activity increased. At high levels of LDLPFC activity, Stroop performance did not vary as a function of dACC activity.

This hierarchical regression was repeated with Stroop errors as the DV. The full model accounted for 9% of the variance, $F(3,76) = 2.58$, $p = .06$. The LDLPFC x dACC interaction contributed 7 % of the variance, $t(76) = .02$ (see Figure 5b), and the model was only significant when the interaction was included. As with Stroop interference for RT, the Stroop error rate was insensitive to dACC activity when LDLPFC was more active, $t(76) = 1.25$, $p = .21$. When LDLPFC was less active, Stroop errors were reduced when dACC activity was high, but errors increased when dACC activity was low, $t(76) = −2.24$, $p = .03$. In summary, for both performance scores, dACC activity did not impact performance provided that LDLPFC was sufficiently active. When LDLPFC was less active, more active dACC was

associated with slower but more accurate performance, and less active dACC was associated with faster, but less accurate performance.

The hypothesis that late dACC activity is related to response-related processing was tested with a MANOVA conducted with condition (congruent dACC score, incongruent dACC score) and dACC temporal course (220 ms to 340 ms, 520 ms to 680 ms) as factors. Temporal course, $F(1, 79) = 8.21$, $p = .01$, and condition x temporal course, $F(1, 79) = 7.95$, $p = .01$, effects emerged. These effects are apparent in Figure 4b. Pairwise comparisons confirmed that, although there was more activity during the earlier time window ($p = .01$), the conditions differed only during the later time window (incongruent amplitude > congruent amplitude, $p = .02$). Incongruent late dACC amplitude was correlated with Stroop interference, $r(78) = .22$, $p = .02$, whereas incongruent early dACC amplitude was not, $r(78) = .02$, $p = .42$. In order to evaluate whether dACC was the only relevant region in the model to distinguish conditions, a MANOVA with LDLPFC condition (congruent LDLPFC score, incongruent LDLPFC score) was also conducted. Results were marginally significant, (congruent amplitude > incongruent amplitude; $F(1,79) = 3.68$, $p = .06$). Since LDLPFC was not expected to differentiate conditions, this marginal result is treated as a null finding. In summary, results supported a role only for late dACC activity in differentiating Stroop conditions, which is consistent with the hypothesis that dACC (and not LDLPFC) has a direct relationship with response-related processing. Furthermore, this finding indicates that response-related processes are occurring after LDLPFC has been activated.

In order to test the specificity of the temporal course of regional brain activity proposed by the cascade model, three additional analyses were conducted to rule out alternative temporal courses and brain networks. A model with early dACC activity (220 ms to 340 ms) and LDLPFC activity (300 ms to 440 ms) was evaluated (Model 2, Table 2). The mediation analysis found no significant paths, the overall regression model was not significant, and the indirect effects were not significant. To rule out the possibility that later dACC activity rather than preceding LDLPFC activity directly predicted greater Stroop interference simply due to the possibility that brain events that occur temporally close to a behavioral response are more related to the behavioral response, LDLPFC and dACC source waveforms were rescored using complementary time windows. Specifically, dACC was scored at 300 ms to 440 ms, and LDLPFC was scored at 520 ms to 620 ms (Model 3, Table 2). This dACC score was the IV, the late LDLPFC score was the M, and Stroop interference was the DV. Similar to the results for Model 2 (Table 2), there were no significant path or mediation effects for this model, indicating that the significant effects in Model 1 supporting the cascade model were not merely due to the greater proximity of the late dACC activity relative to the overt response.

The possibility that the mediation of LDLPFC activity provided by subsequent dACC activity was not specific to earlier LDLPFC activity was also examined. RIFG activity (scored 300 ms to 460 ms, based on examination of the grand-average source RIFG waveform) was entered into a mediation model as the IV. Late dACC was entered as the M, and Stroop interference score was the DV. RIFG was specifically selected for this analysis because it has been repeatedly implicated in tasks involving prepotent inhibition and cognitive control (for review see Aron, Robbins, & Poldrack, 2004). This model was not

significant (see Model 4, Table 2), providing evidence for the specificity of the relationship between LDLPFC and subsequent dACC activity during Stroop performance.

Discussion

Although it has been repeatedly shown that LDLPFC and dACC work in conjunction as part of a frontocingulate network, few studies have explicitly investigated the time course of their activity. This is apparently the first study to combine fMRI and EEG methods to study the temporal dynamics of these regions during top-down attentional control. Results indicated that LDLPFC activity influenced Stroop performance via its relationship with later dACC activity, consistent with the temporal course hypothesis posited by the cascade-of-control model. The relationship between dACC activity and Stroop performance was dependent on the level of earlier LDLPFC activity. Further supporting the cascade model, only later dACC activity distinguished between incongruent/congruent conditions, demonstrating that late-stage selection processes are specifically associated with dACC function.

Present evidence that LDLPFC and dACC work in conjunction is consistent with the commonly reported observation that PFC is co-activated with ACC during tasks that require top-down attentional control (Botvinick et al., 2001; Bush et al., 2000; Hanslymayr et al., 2008; Koski & Paus, 2000; MacDonald et al., 2000). A large meta-analysis of neuroimaging studies showed that the pattern of PFC-ACC co-activations is independent of stimulus and response modalities (Koski & Paus, 2000), suggesting that the coupling between these two regions is particularly important. The functional evidence for a frontocingulate network is supported by neuroanatomical findings showing that PFC projects to and receives information from ACC, particularly via association fibers in the cingulum bundle (Barbas, 1992; Petrides & Pandya, 1999).

Present results provide additional insights into the relationship between these two structures. The mediation analyses demonstrated that the degree to which dACC influenced Stroop performance depended on the level of earlier LDLPFC activity. When LDLPFC activity levels were high, there was little impact of dACC activity on Stroop performance, suggesting that, when LDLFPC provides sufficient attentional control, dACC plays a smaller role in affecting overt performance. However, in the context of relatively low LDLPFC activity, dACC activity affected Stroop performance in ways consistent with the cascade-of-control model. Under these conditions, relatively high dACC activity was associated with a response pattern that involved slow responses and few errors. The lower error rate suggests that dACC activity can indeed compensate for poor top-down control by LDFLPC. Consistent with the idea that dACC aids late-stage selection by "picking up the slack" for poor top-down guidance by LDLPFC, responses under these conditions are elongated, presumably because more time is required to resolve interference. Conversely, low dACC activity was related to relatively fast responses with more errors. This finding suggests that, when dACC does not pick up the slack for poor top-down control by LDLPFC, errors are more likely. Because dACC has played a relatively small role in resolving interference between competing aspects of information, responses are made quickly.

Present results provide more direct evidence for the suggestion that on attentionally-demanding tasks, dACC activity increases when LDLPFC activity is relatively low. In prior

studies, increased activity in dACC during a color-word Stroop task was associated with decreased LDLPFC activity in older adults, moreso than in younger adults (Milham et al., 2002). The authors suggested that increased response conflict in the context of reduced top-down attentional control (less efficient maintenance of task set) caused a need for increased dACC activity in order to maintain adequate task performance. The Milham et al. (2002) study provided only indirect evidence for such a relationship between DLPFC and dACC, because it involved a comparison of patterns of activation across two groups. The results obtained in the present study are important because they provide more direct evidence from variations in performance from trial-to-trial, within the same individuals, that LDLPFC and dACC function as closely linked processors whose activity is modulated in an adaptive manner.

The finding that dACC activity was not critical for performance when DLPFC activity was high is also consistent with prior studies. In one experiment (Milham, Banich, Claus, & Cohen, 2003), participants were taught an association that induced a Stroop-like interference effect, but one that dissipates over time. In the beginning, when there was a need to resolve interference, both DLPFC and dACC showed high activity. With practice, and reduced interference, DLPFC activity remained high, but dACC activity dropped drastically. This pattern was interpreted to suggest that, as DLPFC control improves, the need for the dACC to aid in late-stage selection is reduced.

As prior research has suggested that the relationship between DLPFC and dACC varies for different groups of individuals, such as older versus younger adults, it is of interest to consider how this relationship might also vary for those with a history of past or ongoing psychopathology symptoms or diagnoses (Levin et al., 2007). For example, bilateral DLPFC, dACC, rostral ACC, and subgenual ACC (Cg25) are robustly identified brain regions affected in depression, and depression has been theorized to be related to abnormal functional interactions among a larger network of limbic-cortical regions (Ressler & Mayberg, 2007). Future studies using neuroimaging methods with high temporal and spatial resolution in clinical samples are likely to be able to shed further light on the interrelationship between the DLPFC and dACC. Such studies have the potential to influence intervention and treatment strategies for depression, as well as to inform the advancement of theories regarding cognitive control and the associated temporal course related to frontocingulate activity.

An aspect of present findings that was not entirely clear was the nature of the early activity observed for dACC around 200 ms. Of note, this activity did not differentiate congruent and incongruent trials, nor was it related to overt behavior in the form of Stroop interference. Therefore, it does not appear to be related to the degree of attentional control that must be exerted on a given trial. One possibility is that some of the variance in the signal being picked up at this dACC source reflects activity in pre-SMA, which may provide a top-down bias toward task-relevant stimulus-response mapping i.e., the response mapping of each finger to each color (Donohue, Wendelken, & Bunge, 2008; Hoshi & Tanji, 2004). This explanation would be consistent with a lack of differentiation between congruent and incongruent trials for this early component, as such response mappings do not vary

depending on the nature of the trial. Understanding the function reflected by this early dACC component remains an issue for future research.

Summary

Present analyses utilized integrated fMRI/EEG methods, a well-studied task of cognitive control (the color-word Stroop task), multiple manipulation checks, and diverse analytic strategies to test and confirm a pattern of temporal dynamics consistent with the directionality predicted by the cascade-of-control model. As predicted, response-related processes were specifically related to later dACC activity but not to earlier dACC or LDLPFC activity. The extent to which dACC activity influenced Stroop performance depended on the degree of earlier LDLPFC activity, demonstrating an interdependent relationship among these brain regions. Different behavioral patterns emerged based on the levels of observed LDLPFC activity. Consistent with the cascade-of-control model, when levels of LDLPFC activity were high, the level of dACC activity did not affect performance, presumably because the top-down control imposed by LDLPFC allowed for adequate performance. However, when LDLPFC activity levels were low, high dACC activity was associated with better performance and elongated reaction time, consistent with the idea that dACC was compensating for the lack of top-down LDLFPC control. In contrast, when dACC activity was low, a higher error rate and faster responding were observed, suggesting that dACC did not compensate for the lack of top-down control. These findings advance understanding about the temporal directionality of activity within the frontal regions involved in exerting top-down attentional control.

Acknowledgments

References

Aron AR, Robbins TW, Poldrack RA. Inhibition and the right inferior frontal cortex. Trends in Cognitive Sciences. 2004; 8:170–177. [PubMed: 15050513]

Aguirre GK, Zarahn E, D'Esposito M. The variability of human BOLD hemodynamic response. NeuroImage. 1998; 8:360–369. [PubMed: 9811554]

Badzakova-Trajkov, Barnett KJ, Waldie KE, Kirk IJ. An ERP investigation of the Stroop task: The role of the cingulate in attentional allocation and conflict resolution. Brain Research. 2009; 1253:139–148. [PubMed: 19084509]

Banich MT, Milham MP, Atchley R, Cohen NJ, Webb A, Wszalek T, et al. fMRI studies of stroop tasks reveal unique roles of anterior and posterior brain systems in attentional selection. Journal of Cognitive Neuroscience. 2000a; 12:988–1000. [PubMed: 11177419]

Banich MT, Milham MP, Atchley RA, Cohen NJ, Webb A, Wszalek T, et al. Prefrontal regions play a predominant role in imposing an attentional 'set': Evidence from fMRI. Cognitive Brain Research. 2000b; 10:1–9. [PubMed: 10978687]

Banich MT. Executive function: The search for an integrated account. Current Directions in Psychological Science. 2009; 18:89–94.

Banich MT, Mackiewicz KL, Depue BE, Whitmer A, Miller GA, Heller W. Cognitive control mechanisms, emotion, & memory: A neural perspective with implications for psychopathology. Neuroscience and Biobehavioral Reviews. 2009; 33:613–630. [PubMed: 18948135]

Barbas, H. Architecture and cortical connections of the prefrontal cortex in the rhesus monkey. In: Chauvel, P.Delgado-Escueta, AV.Halgren, E., Bancaud, J., editors. Advances in neurology. New York: Raven Press; 1992. p. 91-115.

Bench CJ, Frith CD, Grasby PM, Friston KJ, Paulesu E, Frackowiak RS, et al. Investigations of the functional anatomy of attention using the Stroop test. Neuropsychologia. 1993; 31:907–922. [PubMed: 8232848]

Berg P, Scherg M. A multiple source approach to the correction of eye artifacts. Electroencephalography and Clinical Neurophysiology. 1994; 90:229–241. [PubMed: 7511504]

Blanco C, Okuda M, Wright C, Hasin DS, Grant BF, Liu S, Olfson M. Mental health of college students and their non-college attending peers: Results from the national epidemiologic study on alcohol and related conditions. Archives of General Psychiatry. 2008; 65:1429–1437. [PubMed: 19047530]

Botvinick MM, Braver TS, Barch DM, Carter CS, Cohen JD. Conflict monitoring and cognitive control. Psychological Review. 2001; 108:624–652. [PubMed: 11488380]

Botvinick MM, Cohen JD, Carter CS. Conflict monitoring and anterior cingulate cortex: An update. Trends in Cognitive Sciences. 2004; 8:539–546. [PubMed: 15556023]

Brody AL, Saxena S, Stoessel P, Gillies LA, Fairbanks LA, Alborzian S, Phelps ME, et al. Regional brain metabolic changes in patients with major depression treated with either paroxetine or interpersonal therapy. Archives of General Psychiatry. 2001; 58:631–640. [PubMed: 11448368]

Buschman TJ, Miller EK. Top-down versus bottom-up control of attention in the prefrontal and posterior parietal cortices. Science. 2007; 315:1860–1862. [PubMed: 17395832]

Bush G, Luu P, Posner MI. Cognitive and emotional influences in anterior cingulate cortex. Trends in Cognitive Sciences. 2000; 4:215–222. [PubMed: 10827444]

Carter CS, Mintun M, Cohen JD. Interference and facilitation effects during selective attention: An H215O PET study of stroop task performance. NeuroImage. 1995; 2:264–272. [PubMed: 9343611]

Carter CS, Botvinick MM, Cohen JD. The contribution of the anterior cingulate cortex to executive processes in cognition. Reviews in the Neurosciences. 1999; 10:49–57. [PubMed: 10356991]

Cheung GW, Lau RS. Testing mediation and suppression effects of latent variables: Bootstrapping with structural equation models. Organizational Research Methods. 2008; 11:296–325.

Cohen J. A power primer. Psychological Bulletin. 1992; 112:155–159. [PubMed: 19565683]

Cohen JD, Botvinick M, Carter CS. Anterior cingulate and prefrontal cortex: Who's in control? Nature Neuroscience. 2000; 3:421–423. [PubMed: 10769376]

Cook EW, Miller GA. Digital filtering: Background and tutorial for psychophysiologists. Psychophysiology. 1992; 29:350–367. [PubMed: 1626044]

Donohue SE, Wendelken C, Bunge SA. Neural correlates of preparation for action selection as a function of specific task demands. Journal of Cognitive Neuroscience. 2008; 20:694–706. [PubMed: 18052782]

Donkers FC, van Boxtel GJ. The N200 in go/no-go tasks reflects conflict monitoring not response inhibition. Brain and Cognition. 2004; 56:165–176. [PubMed: 15518933]

Edgar, JC., Stewart, JL., Miller, GA. Digital filtering in EEG/ERP research. In: Handy, TC., editor. Event-related potentials: A handbook. Cambridge, MA: MIT Press; 2005. p. 85-113.

Fan J, Flombaum JI, McCandliss BD, Thomas KM, Posner MI. Cognitive and brain consequences of conflict. NeuroImage. 2003; 18:42–57. [PubMed: 12507442]

First, MB., Spitzer, RL., Gibbon, M., Williams, JBW. Structured clinical interview for DSM-IV axis I disorders – non-patient edition (SCID-I/NP, version 2.0 – 4/97 revision). New York: Biometrics Research Department; 1997.

Garavan H, Ross TJ, Kaufman J, Stein EA. A midline dissociation between error-processing and response-conflict monitoring. NeuroImage. 2003; 20:1132–1139. [PubMed: 14568482]

Hanslmayr S, Pastötter B, Bäuml K-H, Gruber S, Wimber M, Klimesch W. The electrophysiological dynamics of interference during the Stroop task. Journal of Cognitive Neuroscience. 2008; 20:215–224. [PubMed: 18275330]

Harvey PO, Fossati P, Pochon JB, Levy R, Lebastard G, Lehericy S, et al. Cognitive control and brain resources in major depression: An fMRI study using the n-back task. NeuroImage. 2005; 26:860–869. [PubMed: 15955496]

Herrington JD, Heller W, Mohanty A, Engels A, Banich MT, Webb AW, Miller GA. Localization of asymmetric brain function in emotion and depression. Psychophysiology. In press.

Holmes AJ, Pizzagalli DA. Response conflict and frontocingulate dysfunction in unmedicated participants with major depression. Neuropsychologia. 2008; 46:2904–2913. [PubMed: 18577391]

Holroyd, CB. A note on the N200 and the feedback ERN. In: Ullsperger, M., Falkenstein, M., editors. Errors, conflicts, and the brain: Current opinions on performance monitoring. Leipzig, Germany: MPI of Cognitive Neuroscience; 2004. p. 211-218.

Hoshi E, Tanji J. Differential roles of neuronal activity in the supplementary and presupplementary motor areas: From information retrieval to motor planning and execution. Journal of Neurophysiology. 2004; 92:3482–3499. [PubMed: 15269227]

Jackson SR, Jackson GM, Roberts M. The selection and suppression of action: ERP correlates of executive control in humans. Neuroreport. 1999; 10:861–865. [PubMed: 10208561]

Jenkinson M, Bannister P, Brady M, Smith S. Improved optimization for the robust and accurate linear registration and motion correction of brain images. NeuroImage. 2002; 17:825–841. [PubMed: 12377157]

Kennedy SH, Evans KR, Kruger S, Mayberg HS, Meyer JH, McCann S, Arifuzzman AI, et al. Changes in regional brain glucose metabolism measured with positron emission tomography after paroxetine treatment of major depression. American Journal of Psychiatry. 2001; 158:899–905. [PubMed: 11384897]

Kerns JG, Cohen JD, MacDonald AW III, Cho RY, Stenger VA, Carter CS. Anterior cingulate conflict monitoring and adjustments in control. Science. 2004; 303:1023–1026. [PubMed: 14963333]

Kiefer M, Marzinzik F, Weisbrod M, Scherg M, Spitzer M. The time course of brain activations during response inhibition: Evidence from event-related potentials in a go/no go task. Neuroreport. 1998; 9:765–770. [PubMed: 9559953]

Koski L, Paus T. Functional connectivity of the anterior cingulate cortex within the human frontal lobe: A brain-mapping meta-analysis. Experimental Brain Research. 2000; 133:55–65. [PubMed: 10933210]

Kutas M, Hillyard SA. Reading senseless sentences: brain potentials reflect semantic incongruity. Science. 1980; 207:203–205. [PubMed: 7350657]

Liotti M, Woldorff MG, Perez R, Mayberg HS. An ERP study of the temporal course of the stroop color-word interference test. Neuropsychologia. 2000; 38:701–711. [PubMed: 10689046]

Liu X, Banich MT, Jacobson BL, Tanabe JL. Functional dissociation of attentional selection within PFC: Response and non-response related aspects of attentional selection as ascertained by fMRI. Cerebral Cortex. 2006; 16:827–834. [PubMed: 16135781]

Luck, SJ. An Introduction to the Event-Related Potential Technique. London: The MIT Press; 2005.

MacDonald AW 3rd, Cohen JD, Stenger VA, Carter CS. Dissociating the role of the dorsolateral prefrontal and anterior cingulate cortex in cognitive control. Science. 2000; 288:1835–1838. [PubMed: 10846167]

MacKinnon, DP. Introduction to Statistical Mediation Analysis. New York, NY: Tayor & Francis Group; 2008.

Markela-Lerenc J, Ille N, Kaiser S, Fiedler P, Mundt C, Weisbrod M. Prefrontal-cingulate activation during executive control: Which comes first? Cognitive Brain Research. 2004; 18:278–287. [PubMed: 14741314]

Meyer TJ, Miller ML, Metzger RL, Borkovec TD. Development and validation of the penn state worry questionnaire. Behavior Research and Therapy. 1990; 28:487–495.

Michel CM, Murray MM, Lantz G, Gonzalez S, Spinelli L, Grave de Peralta R. EEG source imaging. Clinical Neurophysiology. 2004; 115:2195–2222. [PubMed: 15351361]

Miezin FM, Maccotta L, Ollinger JM, Petersen SE, Buckner RL. Characterizing the hemodynamic response: Effects of presentation rate, sampling procedure, and the possibility of ordering brain activity based on relative thinking. Neuroimage. 2000; 11:735–739. [PubMed: 10860799]

Milham MP, Banich MT. Anterior cingulate cortex: An fMRI analysis of conflict specificity and functional differentiation. Human Brain Mapping. 2005; 25:328–335. [PubMed: 15834861]

Milham MP, Banich MT, Barad V. Competition for priority in processing increases prefrontal cortex's involvement in top-down control: An event-related fMRI study of the stroop task. Cognitive Brain Research. 2003; 17:212–222. [PubMed: 12880892]

Milham MP, Banich MT, Claus ED, Cohen NJ. Practcice-related effects demonstrate complementary roles of anterior cingulated and prefrontal cortices in attentional control. NeuroImage. 2003; 18:483–493. [PubMed: 12595201]

Milham MP, Erickson KI, Banich MT, Kramer AF, Webb A, Wszalek T, Cohen NJ. Attentional control in the aging brain: Insight from an fMRI study of the Stroop task. Brain and Cognition. 2001; 49:277–296.

Miller EK, Cohen JD. An integrative theory of prefrontal cortex function. Annual Review of Neuroscience. 2001; 24:167–202.

Miller GA, Gratton G, Yee CM. Generalized implementation of an eye movement correction procedure. Psychophysiology. 1988; 25:241–243.

Mohanty A, Engels AS, Herrington JD, Heller W, Ho MR, Banich MT, et al. Differential engagement of anterior cingulate cortex subdivisions for cognitive and emotional function. Psychophysiology. 2007; 44:343–351. [PubMed: 17433093]

Molina, S., Borkovec, TD. The Penn state worry questionnaire: Psychometric properties and associated characteristics. In: Davey, GCL., Tallis, F., editors. Worrying: Perspectives on Theory, Assessment and Treatment. Chichester: Wiley; 1994. p. 265-283.

Nitschke JB, Heller W, Imig JC, McDonald RP, Miller GA. Distinguishing dimensions of anxiety and depression. Cognitive Therapy and Research. 2001; 25:1–22.

Nitschke JB, Miller GA, Cook EW III. Digital filtering in EEG/ERP analysis: Some technical and empirical comparisons. Behavior Research Methods, Instruments & Computers. 1998; 30:54–67.

Oldfield RC. The assessment and analysis of handedness: The edinburgh inventory. Neuropsychologia. 1971; 9:97–113. [PubMed: 5146491]

Petrides M, Pandya DN. Dorsolateral prefrontal cortex: Comparative cytoarchitectonic analysis in the human and the macaque brain and corticocortical connection patterns. The European Journal of Neuroscience. 1999; 11:1011–1036. [PubMed: 10103094]

Pardo JV, Pardo PJ, Janer KW, Raichle ME. The anterior cingulate cortex mediates processing selection in the stroop attentional conflict paradigm. Proceedings of the National Academy of Sciences. 1990; 87:256–259.

Perrin F, Pernier J, Bertran D. Spherical splines for scalp potential and current density mapping. EEG and Clinical Neurophysiology. 1989; 72:184–187.

Preacher KJ, Hayes AF. SPSS and SAS procedures for estimating indirect effects in simple mediation models. Behavior Research methods, Instruments, & Computers. 2004; 36:717–731.

Preacher KJ, Hayes AF. Asymptotic and resampling strategies for assessing and comparing indirect effects in multiple mediator models. Behavior Research Methods. 2008; 40:879–891. [PubMed: 18697684]

Ressler KJ, Mayberg HS. Targeting abnormal circuits in mood and anxiety disorders: From the laboratory to the clinic. Nature Neuroscience. 2007; 9:1116–1124.

Sobel ME. Asymptotic confidence intervals for indirect effects in structural equation models. Sociological Methodology. 1982; 13:290–312.

Stroop JR. Factors affecting speed in serial verbal reactions. Journal of Experimental Psychology. 1935; 18:643–662.

van Veen V, Carter CS. The timing of action-monitoring processes in anterior cingulate cortex. Journal of Cognitive Neuroscience. 2002; 14:593–602. [PubMed: 12126500]

Ward, DB. [accessed July 27, 2006] Simultaneous inference for FMRI data. 2000. http://afni.nimh.nih.gov/pub/dist/doc/manual/AlphaSim.pdf

Watson D, Clark LA, Weber K, Assenheimer JS, Strauss ME, McCormick RA. Testing a tripartite model: II. exploring the symptom structure of anxiety and depression in student, adult, and patient samples. Journal of Abnormal Psychology. 1995a; 104:15–25. [PubMed: 7897037]

Watson D, Weber K, Assenheimer JS, Clark LA, Strauss ME, McCormick RA. Testing a tripartite model: I. evaluating the convergent and discriminant validity of anxiety and depression symptom scales. Journal of Abnormal Psychology. 1995b; 104:3–14. [PubMed: 7897050]

West R. Neural correlates of cognitive control and conflict detection in the stroop and digit-location tasks. Neuropsychologia. 2003; 41:1122–1135. [PubMed: 12667546]

West R, Bowry R, McConville C. Sensitivity of medial frontal cortex to response and nonresponse conflict. Psychophysiology. 2004; 41:739–748. [PubMed: 15318880]

Woolrich MW, Ripley BD, Brady M, Smith S. Temporal autocorrelation in univariate linear modeling of fMRI data. NeuroImage. 2001; 14:1370–1386. [PubMed: 11707093]

Yeung N, Botvinick M, Cohen JD. The neural basis of error detection: Conflict monitoring and the error-related negativity. Psychological Review. 2004; 111:931–959. [PubMed: 15482068]
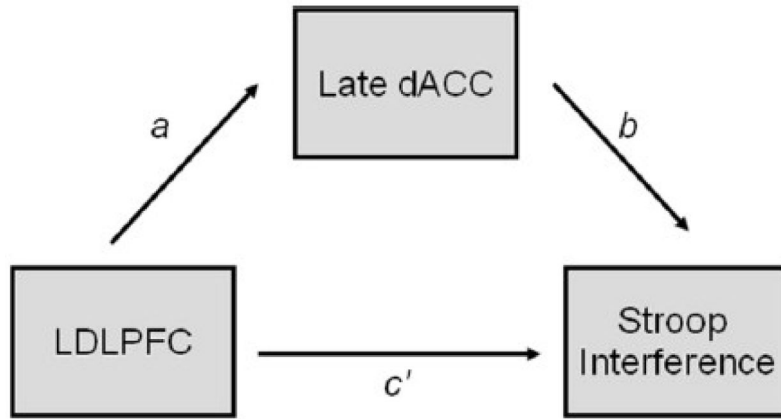
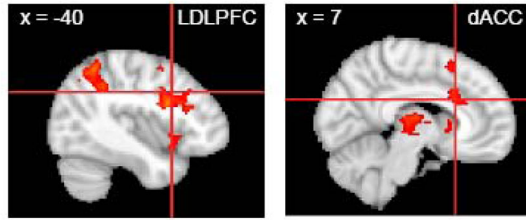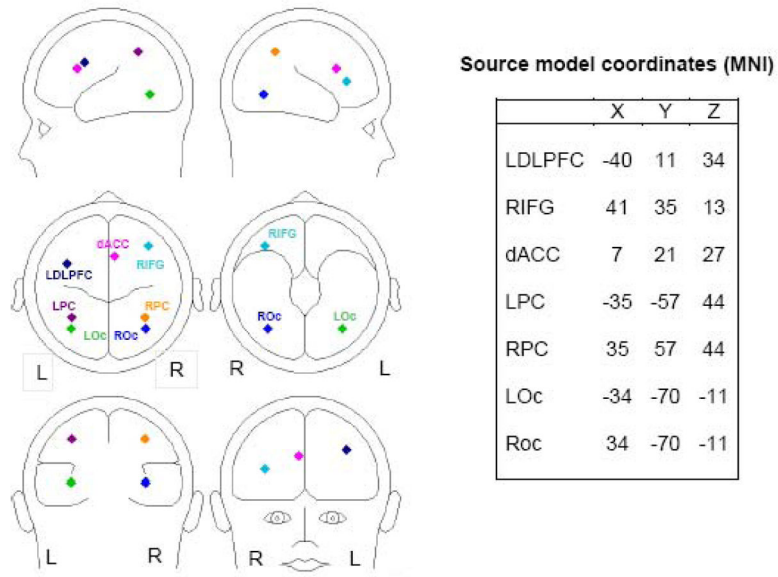**Cascade-of-Control Model**

Figure 1.
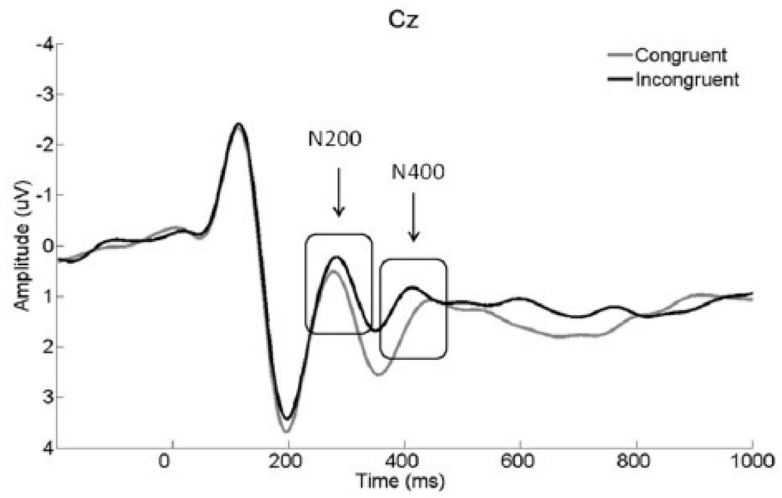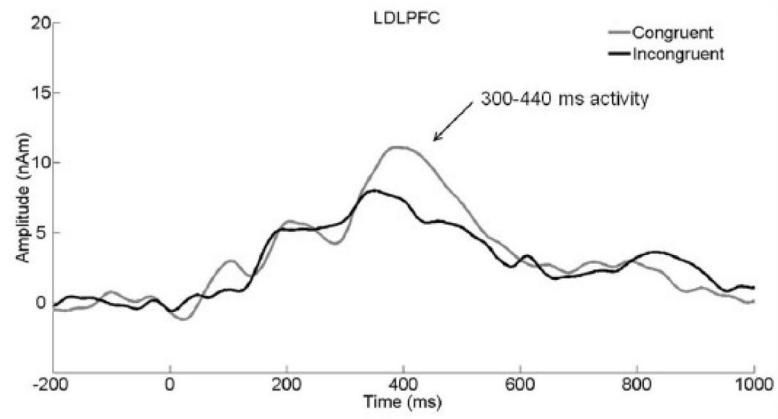
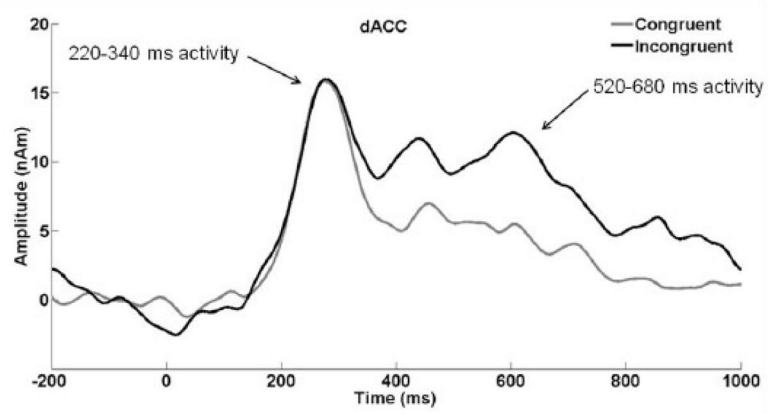Figure 2a.

Figure 2b.

Figure 2.

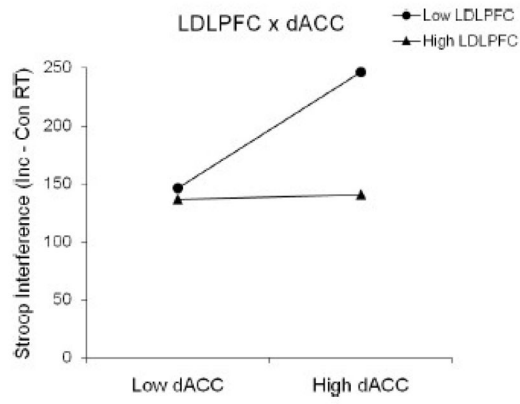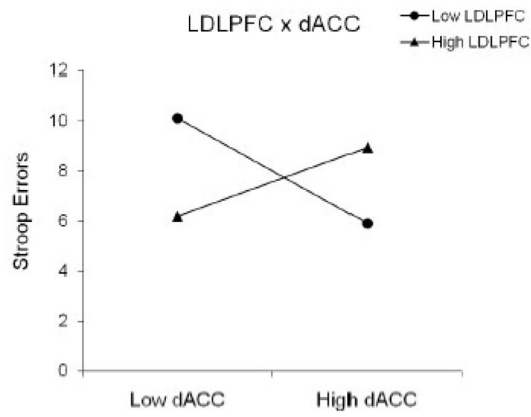**Figure 3.**

Figure 4a.

Figure 4b.

Figure 4.

Figure 5a.

Figure 5b.

Figure 5.

Table 1

fMRI Center of Mass coordinates (MNI)

Region	Cluster Size	Mean Z	X	Y	Z
Left Frontal Orbital Cortex	545	3.76	−31	19	−8
Right Frontal Orbital Cortex	749	3.61	36	21	−6
Left Inferior Temporal Gyrus	36	3.36	−53	−56	−15
Left Intracalcarine Cortex	111	3.39	−8	−79	2
Right Thalamus	1126	3.61	0	−16	7
Right Caudate	67	3.28	11	11	7
Left Putamen	37	3.31	−23	−2	9
Right Inferior Frontal Gyrus (RIFG) *	42	3.35	41	35	13
Left Precentral Gyrus (LDLPFC) *	1195	3.72	−40	11	34
Right Anterior Cingulate Gyrus (dACC) *	182	3.50	7	21	27
Left Lateral Occipital Cortex (LPC) *	1376	3.77	−35	−57	44
Left Precuneus Cortex	443	3.61	−5	−63	45
Paracingulate Gyrus	335	3.54	0	14	51
Right Superior Parietal Lobule	132	3.49	39	−50	48

*
Brain regions used in source analysis (see Figure 2)

Author Manuscript   Author Manuscript   Author Manuscript   Author Manuscript

Table 2

Summary of mediation analyses

Model	Path a	Path b	Path c	Path c′	Indirect Effect (a x b)	Regression Summary(R^2)
1. Model 1 (Cascade model)	.34[*]	1.86[*]	−1.41	−2.00[*]	.63[a]	.09[*]
2. Model 2 (early dACC, late LDLPFC)	.13	−1.24	−.75	.38	−.16	.03
3. Model 3 (revised scoring)	.05	.41	−.69	−.71	.02	.01
4. Model 4 (RIFG substituted for LDLPFC)	.48[*]	1.45	1.86	1.16	.70	.08[*]

Note. Table entries in middle five columns are path coefficients

[*]
$p < .05$

[a]Significant point estimate ($p < .05$), 95% BCa CI = .01 to 1.82, $k = 5000$